

# A dominant-negative mutation in the TRESK potassium channel is linked to familial migraine with aura

Ronald G Lafrenière<sup>1,2,13</sup>, M Zameel Cader<sup>3,4,13</sup>, Jean-François Poulin<sup>2</sup>, Isabelle Andres-Enguix<sup>5</sup>, Maryse Simoneau<sup>2</sup>, Namrata Gupta<sup>2</sup>, Karine Boisvert<sup>2</sup>, François Lafrenière<sup>2</sup>, Shannon McLaughlan<sup>2</sup>, Marie-Pierre Dubé<sup>6</sup>, Martin M Marcinkiewicz<sup>7</sup>, Sreeram Ramagopalan<sup>8</sup>, Olaf Ansorge<sup>9</sup>, Bernard Brais<sup>1</sup>, Jorge Sequeiros<sup>10</sup>, Jose Maria Pereira-Monteiro<sup>11</sup>, Lyn R Griffiths<sup>12</sup>, Stephen J Tucker<sup>5</sup>, George Ebers<sup>8</sup> & Guy A Rouleau<sup>1,2</sup>

**Migraine with aura is a common, debilitating, recurrent headache disorder associated with transient and reversible focal neurological symptoms<sup>1</sup>. A role has been suggested for the two-pore domain (K2P) potassium channel, TWIK-related spinal cord potassium channel (TRESK, encoded by *KCNK18*), in pain pathways and general anaesthesia<sup>2</sup>. We therefore examined whether TRESK is involved in migraine by screening the *KCNK18* gene in subjects diagnosed with migraine. Here we report a frameshift mutation, F139WfsX24, which segregates perfectly with typical migraine with aura in a large pedigree. We also identified prominent TRESK expression in migraine-salient areas such as the trigeminal ganglion. Functional characterization of this mutation demonstrates that it causes a complete loss of TRESK function and that the mutant subunit suppresses wild-type channel function through a dominant-negative effect, thus explaining the dominant penetrance of this allele. These results therefore support a role for TRESK in the pathogenesis of typical migraine with aura and further support the role of this channel as a potential therapeutic target.**

Migraine is a common recurrent headache disorder, with an annual prevalence estimated at 18.2% in females and 6.5% in males<sup>1</sup>. One third of attacks, which can last from 4 to 72 h, are preceded by transient neurological disturbances known as aura. These are commonly visual, taking the form of scintillating shapes, hallucinations or black spots. Cortical spreading depression (CSD) underlies the aura, and, although its precise relationship to headache is unclear, there is evidence in rats that CSD can activate trigeminal nociceptors<sup>3,4</sup>. During a migraine headache, trigeminal ganglion nerve afferents innervating the meningeal nociceptors secrete pro-inflammatory peptides (such as CGRP and substance P) that cause local inflammation, intensify activation

of the trigeminal ganglion afferents<sup>5</sup> and may lead to central sensitization. Considerable insights into the pathogenesis of migraine have come from the investigation of the rare autosomal dominant subtype of migraine with aura, familial hemiplegic migraine. Three susceptibility genes (*CACNA1A*, *ATP1A2* and *SCN1A*), which encode either ion channels or ion transport proteins, have so far been identified<sup>6–8</sup>, and it is likely that mutations in these genes reduce the threshold for CSD<sup>9,10</sup>. However, such mutations are not found in typical migraine with aura, suggesting that other ion channels may be involved.

K2P channels are expressed throughout the central nervous system and have a key role in controlling neuronal resting membrane potential and neuronal excitability<sup>11</sup>. They represent a major target for many volatile anesthetics and neuroprotective agents and have been implicated in a variety of pain pathways. The TRESK K2P channel, encoded by the *KCNK18* gene, is expressed in spinal cord, where it helps modulate cellular excitability. The channel is directly activated by calcineurin after G<sub>q</sub> receptor stimulation and a subsequent rise in intracellular calcium<sup>12,13</sup>. It is therefore a potential target of pain mediators that exert their action via these pathways, and a role has recently been suggested for TRESK in the calcineurin inhibitor-induced pain syndrome<sup>14,15</sup>. TRESK is also activated by volatile anesthetics such as halothane<sup>16</sup>, which have been shown to inhibit CSD<sup>17</sup>. We therefore decided to examine the potential role of TRESK in typical migraine with aura.

We sequenced the entire coding region of the *KCNK18* gene in a panel of 110 unrelated migraine probands. We identified five sequence variants (**Supplementary Table 1**): one silent mutation (L240L), three missense mutations (R10G, C110R and S231P) and a 2-bp deletion of CT at position c.414–415 (**Fig. 1**), which was predicted to cause a frameshift (F139WfsX24), prematurely truncating the protein to 162 residues. Only the L240L and F139WfsX24 variants were not detected after sequencing of the *KCNK18* gene in a panel of 80 population control samples from the

<sup>1</sup>Centre of Excellence in Neuromics and Department of Medicine, Université de Montréal, Centre Hospitalier de l'Université de Montréal, Research Centre, Notre-Dame Hospital, Montreal, Quebec, Canada. <sup>2</sup>Emerillon Therapeutics, Montreal, Quebec, Canada. <sup>3</sup>Medical Research Council Functional Genomics Unit, Department of Physiology, Anatomy and Genetics, University of Oxford, Oxford, UK. <sup>4</sup>Department of Clinical Neurology, John Radcliffe Hospital, Oxford, UK. <sup>5</sup>Clarendon Laboratory, Department of Physics, University of Oxford, Oxford, UK. <sup>6</sup>Faculty of Medicine, Université de Montréal, Montreal Heart Institute, Montreal, Quebec, Canada. <sup>7</sup>Cytochem, Montreal, Quebec, Canada. <sup>8</sup>Wellcome Trust Centre for Human Genetics, University of Oxford, Oxford, UK. <sup>9</sup>Department of Neuropathology, University of Oxford, Oxford, UK. <sup>10</sup>UnIGENE, Institute for Molecular and Cell Biology, University of Porto, Porto, Portugal. <sup>11</sup>Hospital Santo António, Porto, Portugal. <sup>12</sup>Genomics Research Centre, Griffith Health Institute, Griffith University, Gold Coast, Queensland, Australia. <sup>13</sup>These authors contributed equally to this work. Correspondence should be addressed to G.A.R. (guy.rouleau@umontreal.ca) or M.Z.C. (zameel.cader@dpag.ox.ac.uk).

Received 9 July; accepted 23 August; published online 26 September 2010; doi:10.1038/nm.2216

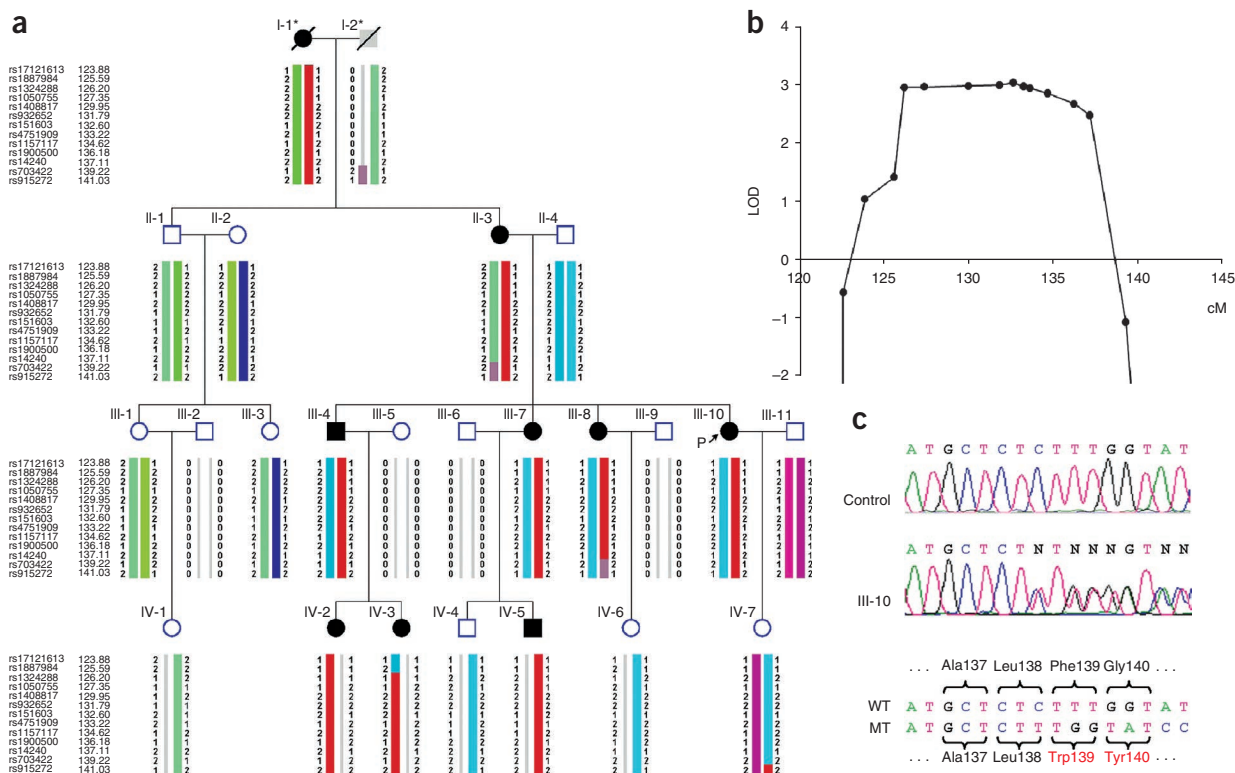


**Figure 1** Segregation analysis in a large migraine with aura pedigree. **(a)** Individuals with clinically confirmed migraine with visual aura are shown as black symbols, unaffected individuals as white symbols and unknown affection as gray. The proband is indicated with an arrow. The haplotypes on 10q25.2–3, covering an indicative 13 of white genotyped SNPs, are shown with different colors to indicate each haplotype; the haplotype segregating with the F139WfsX24 mutation is colored of red. Inferred haplotypes are marked with an asterisk. **(b)** Linkage region overlying 10q25.2–3, with dots representing the following SNP markers: rs1034178, rs17121613, rs1887984, rs1324288, rs1050755, rs1408817, rs932652, rs151603, rs4751909, rs765173, rs1157117, rs1900500, rs14240 and rs703422. LOD, logarithm of the odds ratio; cM, centiMorgan. **(c)** Sequence traces of the c.414–415 CT-deletion mutation predicted to cause a frameshift. MT, mutant allele.

Centre d'Etude du Polymorphisme Humain (CEPH). To further examine whether mutations in *KCNK18* were associated with migraine, we sequenced *KCNK18* in 511 migraine probands from a large Australian cohort and 505 nonmigraine, ethnicity-matched control samples. We thereby identified seven silent (F103F, L143L, Y163Y, S252S, P282P, I289I and T322T) and two missense (A34V and A233V) additional variants. The A233V variant has already been reported in the Single Nucleotide Polymorphism Database (rs363360) and is common (minor allele frequency = 0.15) in African populations. We found the A34V variant in one migraine proband for which family samples were not available.

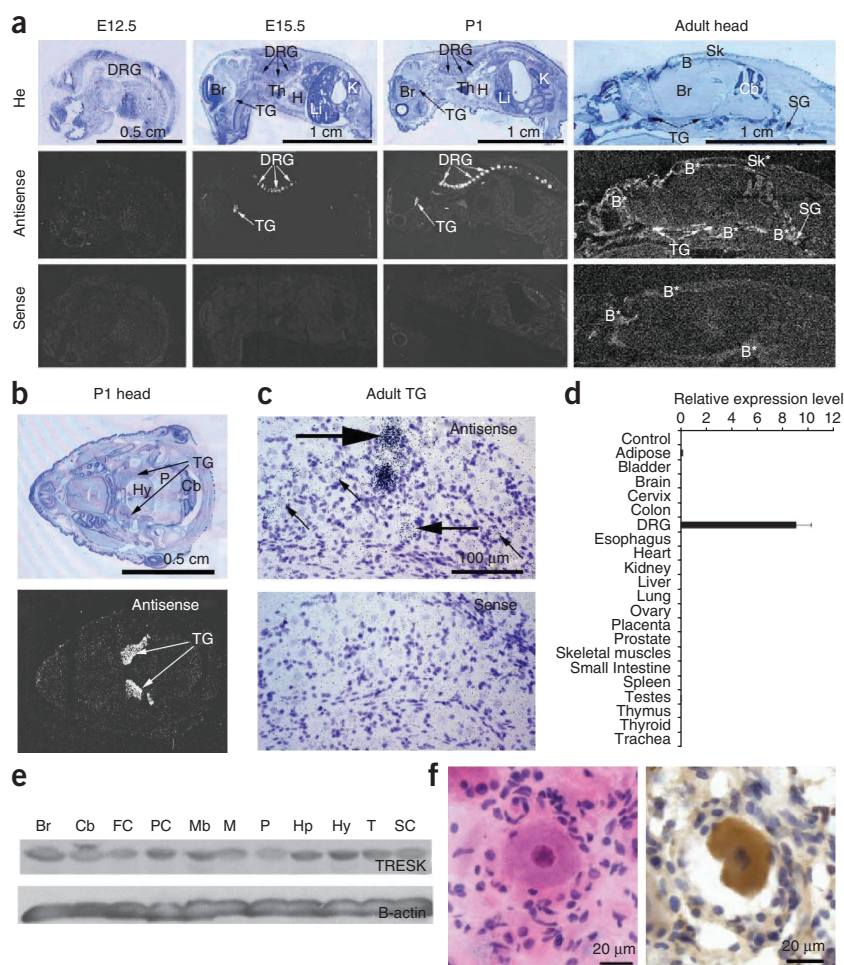
We identified the F139WfsX24 mutation in the large multigenerational family of proband III-10 (**Fig. 1a**) with typical migraine with aura, inherited in a dominant fashion and fully penetrant. Proband III-10 describes a visual aura in the form of bilateral slowly enlarging scotoma with a scintillating edge, typically lasting 20 to 30 min and followed by a throbbing lateralized or holocranial headache. The headache, which lasts 24–48 h, is associated with sensitivity to lights, sounds and smells, as well as nausea and occasional vomiting. The headaches also occur in isolation without a preceding aura. The migraine episodes began in the early teens and triggers included tiredness, alcohol and bright lights. There was no clear association with the menstrual cycle, but after menopause the migraines were less frequent. Other affected individuals in the family describe similar migraine episodes and experience the same aura.

We genotyped 15 additional DNA samples from relatives of the proband, and the F139WfsX24 frameshift mutation segregated perfectly with the eight affected individuals in the pedigree but was absent from the

eight unaffected individuals. This migraine pedigree was part of a larger data set used for a genome-wide linkage screen of microsatellite markers<sup>18</sup>. We reexamined the linkage data but found that the microsatellites used on 10q25.3 were not sufficiently informative to provide useful linkage information (data not shown). We therefore analyzed 141 SNPs genotyped on chromosome 10 in this family, using MERLIN<sup>19</sup> and correcting for linkage disequilibrium between markers. This confirmed a broad linkage region, peaking at 3.03, overlying 10q25.2–3 (**Fig. 1b**). Haplotype mapping defined a crucial linkage region of 13.0 cM (9.7 Mb) with 52 known genes but containing only one identified ion channel gene: *KCNK18*.

We next determined whether TRESK is expressed in areas that are relevant to migraine. We first performed *in situ* hybridization (ISH) analysis to localize the mouse *Kcnk18* mRNA. Although undetectable in embryonic stages, *Kcnk18* expression appeared in trigeminal ganglion and dorsal root ganglia (DRG) from embryonic day 15.5 (E15.5) and increased through E18 to reach a peak in newborn mouse (postnatal day 1 (P1)) (**Fig. 2a,b**). In adult mice, *Kcnk18* expression was highest in trigeminal ganglion (**Fig. 2a**). *Kcnk18* was also expressed in autonomic nervous system ganglia such as the stellate ganglion and paravertebral sympathetic ganglia. Microanalysis showed *Kcnk18* mRNA in a subpopulation of adult stellate ganglion and paravertebral sympathetic ganglia neurons, most likely principal neurons (**Fig. 2c**). In DRG and trigeminal ganglion, *Kcnk18* was expressed in a subpopulation of medium-size and small-size sensory neurons, suggesting expression in both B fibers and C fibers (**Fig. 2c**). We were also able to detect *KCNK18* expression in human tissues, by quantitative RT-PCR, specifically in DRG and not in any of the other 21 tissues tested (**Fig. 2d**). We also

**Figure 2** *KCNK18* and TRESK expression patterns in mice and humans. **(a)** ISH analysis of sagittal whole-body section at E12.5 and E15.5, in a P1 newborn mouse and in an adult mouse head stained with hematoxylin or labeled with an antisense or sense *Kcnk18* riboprobe after 4-d exposure, showing mRNA labeling under dark-field illumination. **(b)** Horizontal section of a newborn (P1) mouse head showing *Kcnk18* expression in the trigeminal ganglion. **(c)** Cross section of adult mouse trigeminal ganglion, with hematoxylin staining. *Kcnk18* antisense probe revealed strongly labeled large size (>35  $\mu$ m) neurons (large arrow), lightly labeled medium size neurons (medium arrow) and lightly labeled small size (>20  $\mu$ m) neurons (small arrows). **(d)** Expression pattern of *KCNK18* in human tissues, as determined by TaqMan quantitative RT-PCR assay normalized to the expression of the human glyceraldehyde 3-phosphate dehydrogenase (*GAPDH*) gene. Data are given as mean values  $\pm$  s.e.m. for three independent experiments. **(e)** Western blotting of adult mouse brain regions with mouse TRESK-specific antibody, showing widespread expression of TRESK in all examined regions of the brain. **(f)** TRESK expression in frozen sections of human trigeminal ganglion. A large ganglion cell with surrounding satellite cells is shown. Staining with TRESK-specific antibody reveals dense cytoplasmic staining. B, bone; Br, brain; Cb, cerebellum; H, heart; He, hematoxylin; Hp, hippocampus; Hy, hypothalamus; K, kidney; Li, liver; M, medulla; Mb, midbrain; P, pons; PC, posterior cortex; SC, spinal cord; SG, stellate ganglion; Sk, skin; T, thalamus; TG, trigeminal ganglion; Th, thymus. The asterisks are meant to indicate the particular location of the indicated tissue type.



assessed the expression of TRESK in neuronal tissue by western blotting and immunohistochemistry. We found TRESK expressed in all adult mouse spinal cord and brain regions, with slightly higher expression in thalamus, hypothalamus, hippocampus and posterior cortex (Fig. 2e). Immunohistochemistry of human tissue revealed strong staining for TRESK in trigeminal ganglion neurons (Fig. 2f). All sizes of neurons expressed TRESK, with staining present throughout the cell body. These findings are consistent with recent descriptions of TRESK expression limited to brain and spinal cord<sup>16,20,21</sup>, with highest expression in DRG<sup>22</sup>. The discrepancy between mRNA and protein expression may be due to the higher sensitivity of the TRESK-specific antibody compared to the ISH probes. However, the fact that we consistently found TRESK expression in the sensory ganglia and trigeminal ganglion suggests that TRESK plays a key part in the excitability of this subset of neurons that are crucial to migraine pathogenesis.

The F139WfsX24 mutation produces a frameshift that prematurely truncates the channel in the second transmembrane domain. To study the functional consequences of this mutation, we characterized the electrophysiological properties of wild-type (WT) and mutant TRESK channels expressed in *Xenopus* oocytes. Oocytes expressing the WT channel showed large, outwardly rectifying whole-cell  $K^+$  currents (Fig. 3a), characteristic of TRESK channel activity<sup>20</sup>. In contrast, we did not observe any such currents in oocytes expressing the F139WfsX24 mutant channel (Fig. 3b). Nonfunctional potassium channel subunits can also assemble with WT subunits, resulting in a dominant-negative suppression of channel activity in the heterozygote<sup>23–25</sup>, an effect that underlies several disease states, including one associated with K2P

channels<sup>26</sup>. When we expressed WT and F139WfsX24 mutant TRESK channels together, there was a dose-dependent reduction of WT current amplitude (Fig. 3c,d). We also examined whether the mutant channels could still be activated by the calcium ionophore ionomycin<sup>12</sup>. Ionomycin treatment induced a large, robust and reversible activation of WT TRESK, but not of the mutant channel (Fig. 3e,f). These results indicate that the truncated F139WfsX24 mutant channel not only is non-functional but also causes a dominant-negative downregulation of WT channel activity. Functional studies in a TRESK-knockout mouse have shown that downregulation of TRESK channel activity *in vivo* results in altered neuronal excitability and therefore represents a probable mechanistic link with the pathogenesis of migraine<sup>22</sup>. Notably, cyclosporin A and FK506 (tacrolimus), two potent immunosuppressants in clinical use that specifically inhibit calcineurin activity and should therefore also inhibit TRESK activation, can increase headache frequency or intensity in organ transplant individuals<sup>27</sup>. The homogeneity of aura symptoms in the present family might also suggest TRESK is involved in aura pathogenesis, perhaps through lowering the CSD threshold. Increasing TRESK activity may therefore protect against migraine, whereas decreasing activity (through *KCNK18* mutations) may increase risk of migraine. Of note, the dominant-negative suppression of TRESK by nonfunctional subunits also leaves a residual current, indicating that agonist-mediated upregulation of this current is a potential therapeutic strategy.

In conclusion, we have used a candidate gene approach and functional analysis to identify a mutation in TRESK that segregates with typical migraine with aura in a large multigenerational family. These results would support a role for other mutations in TRESK to cause similar

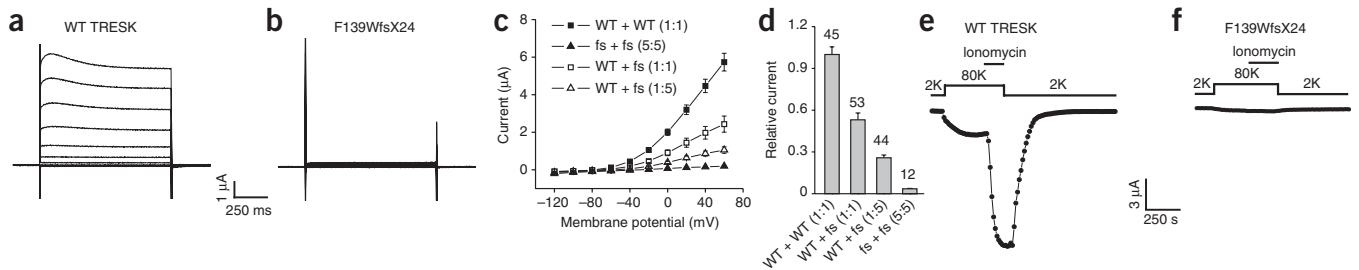


**Figure 3** Electrophysiological characterization of the F139WfsX24 TRESK mutant. (a) Representative currents in 2 mM  $K^+$  from an oocyte expressing WT TRESK. (b) Representative currents in 2 mM  $K^+$  from an oocyte expressing F139WfsX24 mutant TRESK. (c) Dominant-negative effect of coexpression of mutant F139WfsX24 subunits with WT TRESK. Steady-state current-voltage relationships are plotted for the WT TRESK mRNA coexpressed with varying molar ratios of either WT or F139WfsX24 mutant mRNA. The 1:1 WT to WT ratio represents the wild-type state, whereas 1:1 WT to F139WfsX24 (fs) represents the heterozygous state. No currents are observed in the homozygous fs state, even with fivefold overexpression of the F139WfsX24 mRNA (5:5 fs to fs). (d) Quantification of the dominant-negative effects. Peak currents measured at 20 mV and normalized to the average of the control group are plotted for each group. In panels c and d, data are given as mean values  $\pm$  s.e.m. The numbers above the bars represent the number of oocytes measured. (e) Representative response of the WT TRESK to 500 nM ionomycin. (f) Representative response of the F139WfsX24 mutant TRESK to 500 nM ionomycin. As shown above the trace in panels e and f, oocytes were switched from a low  $K^+$  to a high  $K^+$  solution before the application of the  $Ca^{2+}$  ionophore ionomycin, which activates TRESK through a calcineurin-dependent mechanism.

phenotypes, and upregulating TRESK activity with agonists could be of great benefit for migraine sufferers, either as an acute treatment or as a long-term prophylactic.

## METHODS

Methods and any associated references are available in the online version of the paper at <http://www.nature.com/naturemedicine/>.

Note: Supplementary information is available on the Nature Medicine website.

## ACKNOWLEDGMENTS

We thank the subjects and their families for participating in the study and M.K. Charles, M. Albanese, M. Imbeau, A. Anton, S. Meilleur and F. Fernandez for technical assistance. Funding was kindly provided by Genome Canada, Genome Quebec, Emerillon Therapeutics, the Wellcome Trust and Pfizer. M.Z.C. was supported by the Medical Research Council (UK). J.-F.P. was supported by an industrial postdoctoral fellowship from the Natural Sciences and Engineering Research Council of Canada.

## AUTHOR CONTRIBUTIONS

R.G.L. and M.Z.C. planned the experiments and wrote the manuscript. R.G.L. supervised the PCR, dHPLC and sequence analysis, annotated exon and intron structures and verified all data tables and figures. M.Z.C. provided migraine samples, obtained clinical information, performed the linkage analysis and supervised the protein expression studies. M.-P.D. also performed linkage analysis. J.-F.P. supervised PCR, RT-PCR and screening experiments, did DNA sequence analyses and helped write the manuscript. M.S. supervised and performed dHPLC screening experiments and analyses. N.G. supervised PCR and screening experiments. F.L., K.B. and S.M. performed dHPLC and PCR experiments and provided some sequence analysis. M.M.M. conducted the *in situ* hybridization experiments. S.R. helped obtain clinical information and linkage analysis. O.A. supervised the protein expression studies. I.A.-E. and S.J.T. performed the electrophysiology and helped write the manuscript. L.R.G., G.E., B.B., J.S. and J.M.P.-M. provided migraine samples and clinical information. G.A.R. supervised all aspects of the project and edited the manuscript.

## COMPETING FINANCIAL INTERESTS

The authors declare no competing financial interests.

Published online at <http://www.nature.com/naturemedicine/>.

Reprints and permissions information is available online at <http://npg.nature.com/reprintsandpermissions/>.

- Lipton, R.B., Stewart, W.F., Diamond, S., Diamond, M.L. & Reed, M. Prevalence and burden of migraine in the United States: data from the American Migraine Study II. *Headache* **41**, 646–657 (2001).
- Huang, D.Y., Yu, B.W. & Fan, Q.W. Roles of TRESK, a novel two-pore domain  $K^+$  channel, in pain pathway and general anesthesia. *Neurosci. Bull.* **24**, 166–172 (2008).
- Bolay, H. *et al.* Intrinsic brain activity triggers trigeminal meningeal afferents in a migraine model. *Nat. Med.* **8**, 136–142 (2002).

- Zhang, X. *et al.* Activation of meningeal nociceptors by cortical spreading depression: implications for migraine with aura. *J. Neurosci.* **30**, 8807–8814 (2010).
- Iadecola, C. From CSD to headache: a long and winding road. *Nat. Med.* **8**, 110–112 (2002).
- De Fusco, M. *et al.* Haploinsufficiency of *ATP1A2* encoding the  $Na^+/K^+$  pump  $\alpha 2$  subunit associated with familial hemiplegic migraine type 2. *Nat. Genet.* **33**, 192–196 (2003).
- Dichgans, M. *et al.* Mutation in the neuronal voltage-gated sodium channel *SCN1A* in familial hemiplegic migraine. *Lancet* **366**, 371–377 (2005).
- Ophoff, R.A. *et al.* Familial hemiplegic migraine and episodic ataxia type-2 are caused by mutations in the  $Ca^{2+}$  channel gene *CACNL1A4*. *Cell* **87**, 543–552 (1996).
- de Vries, B., Frants, R.R., Ferrari, M.D. & van den Maagdenberg, A.M. Molecular genetics of migraine. *Hum. Genet.* **126**, 115–132 (2009).
- Ramagopalan, S.V., Ramscar, N.E. & Cader, M.Z. Molecular mechanisms of migraine? *J. Neurol.* **254**, 1629–1635 (2007).
- Enyedi, P. & Czirjak, G. Molecular background of leak  $K^+$  currents: two-pore domain potassium channels. *Physiol. Rev.* **90**, 559–605 (2010).
- Czirjak, G., Toth, Z.E. & Enyedi, P. The two-pore domain  $K^+$  channel, TRESK, is activated by the cytoplasmic calcium signal through calcineurin. *J. Biol. Chem.* **279**, 18550–18558 (2004).
- Mathie, A. Neuronal two-pore-domain potassium channels and their regulation by G protein-coupled receptors. *J. Physiol. (Lond.)* **578**, 377–385 (2007).
- Smith, H.S. Calcineurin as a nociceptor modulator. *Pain Physician* **12**, E309–E318 (2009).
- Czirjak, G. & Enyedi, P. Targeting of calcineurin to an NFAT-like docking site is required for the calcium-dependent activation of the background  $K^+$  channel, TRESK. *J. Biol. Chem.* **281**, 14677–14682 (2006).
- Liu, C., Au, J.D., Zou, H.L., Cotten, J.F. & Yost, C.S. Potent activation of the human tandem pore domain K channel TRESK with clinical concentrations of volatile anesthetics. *Anesth. Analg.* **99**, 1715–1722 (2004).
- Piper, R.D. & Lambert, G.A. Inhalational anesthetics inhibit spreading depression: relevance to migraine. *Cephalalgia* **16**, 87–92 (1996).
- Cader, Z.M. *et al.* Significant linkage to migraine with aura on chromosome 11q24. *Hum. Mol. Genet.* **12**, 2511–2517 (2003).
- Abecasis, G.R., Cherny, S.S., Cookson, W.O. & Cardon, L.R. Merlin—rapid analysis of dense genetic maps using sparse gene flow trees. *Nat. Genet.* **30**, 97–101 (2002).
- Sano, Y. *et al.* A novel two-pore domain  $K^+$  channel, TRESK, is localized in the spinal cord. *J. Biol. Chem.* **278**, 27406–27412 (2003).
- Yoo, S. *et al.* Regional expression of the anesthetic-activated potassium channel TRESK in the rat nervous system. *Neurosci. Lett.* **465**, 79–84 (2009).
- Dobler, T. *et al.* TRESK two-pore-domain  $K^+$  channels constitute a significant component of background potassium currents in murine dorsal root ganglion neurons. *J. Physiol. (Lond.)* **585**, 867–879 (2007).
- Wuttke, T.V. *et al.* Peripheral nerve hyperexcitability due to dominant-negative *KCNQ2* mutations. *Neurology* **69**, 2045–2053 (2007).
- Zerr, P., Adelman, J.P. & Maylie, J. Episodic ataxia mutations in *Kv1.1* alter potassium channel function by dominant negative effects or haploinsufficiency. *J. Neurosci.* **18**, 2842–2848 (1998).
- London, B. *et al.* Long QT and ventricular arrhythmias in transgenic mice expressing the N terminus and first transmembrane segment of a voltage-gated potassium channel. *Proc. Natl. Acad. Sci. USA* **95**, 2926–2931 (1998).
- Barel, O. *et al.* Maternally inherited Birk Barel mental retardation dysmorphism syndrome caused by a mutation in the genomically imprinted potassium channel *KCNK9*. *Am. J. Hum. Genet.* **83**, 193–199 (2008).
- Ferrari, U. *et al.* Calcineurin inhibitor-induced headache: clinical characteristics and possible mechanisms. *Headache* **45**, 211–214 (2005).

## ONLINE METHODS

**Clinical samples.** We collected a group of 110 migraine probands as part of ongoing genetic studies in migraine, consisting of 44 subjects from the London, Ontario region diagnosed with migraine with aura as previously reported<sup>18</sup>, 53 subjects of Portuguese origin with migraine as previously reported<sup>28</sup> and 13 subjects of French-Canadian origin with migraine. We used an additional cohort of 511 unrelated migraine probands and 505 ethnicity-matched controls from Australia<sup>29</sup>, collected on the basis of family studies and routine clinical practice. Experienced clinicians specialized in migraine established migraine diagnosis on the basis of International Headache Society criteria<sup>30</sup>. We obtained informed consent from all study participants, and study protocols were approved by the ethics committees of the institutions where collections occurred, in particular the University of Western Ontario Health Sciences Research Ethics Board, the Ethics Committee of the Hospital de Santo António and the Griffith University Ethics Committee for Experimentation on Human Subjects. We used 80 unrelated samples from the Centre d'Etude du Polymorphisme Humain as population controls.

**Screening of the human *KCNK18* gene.** We amplified the three coding exons of the human *KCNK18* gene with four PCR fragments and screened the fragments for DNA variations using a combination of denaturing high-performance liquid chromatography and direct (Sanger) sequencing (see **Supplementary Methods** and **Supplementary Table 2**).

**Single nucleotide polymorphism linkage analysis.** We genotyped 6,090 single nucleotide polymorphisms (SNPs) distributed across the genome with the HumanLinkage-12 Beadchip (Illumina) for samples from proband III-10 and 15 additional family members; 98.1% of SNPs passed quality control filters, yielding a total data set of 5,744 SNPs. Sex chromosome SNPs were not used in the analysis. We had previously identified errors due to sample handling or nonpaternity on a microsatellite genome screen. SNPs on chromosome 10 were analyzed to define the critical linkage region.

**In situ hybridization.** Mouse embryos representing day E0.5, E4.5, E5.5, E6.5, E8.5, E9.5, E12.5, E15.5 and E18, newborn mice (P1 and P10) and whole-body adult mice were frozen, cut into 10- $\mu$ m sections, mounted on glass microscope slides, fixed in formaldehyde and hybridized with <sup>35</sup>S-UTP-labeled cRNA probes, antisense and sense, generating positive and negative (control) signals, respectively. Probes corresponded to a 673-bp fragment from the 3' untranslated region of the *Kcnk18* gene (bp 1,945–2,617 of NM\_207261). After ISH, we analyzed the gene expression patterns by both X-ray film autoradiography (4-d exposure) and emulsion autoradiography (15-d exposure). We viewed lightly hematoxylin-stained sections under either dark-field or bright-field illumination. Cellular level results were revealed at higher microscopic magnification, seen as black labeling by silver grains on a hematoxylin-stained background. ISH assays were performed in accordance with guidelines of the Canadian Council on Animal Care with the approval of the Ethics Committee of the Centre Hospitalier de l'Université de Montréal.

**Quantitative reverse-transcription PCR.** We quantified human *KCNK18* expression by RT-PCR TaqMan assays on a panel of human mRNAs isolated

from various tissues, using *GAPDH* expression as an endogenous control (**Supplementary Methods**).

**Western blotting and immunohistochemistry.** We obtained mouse brain section and spinal cord lysate crude membrane fractions by homogenization in RIPA lysis buffer (50 mM Tris-HCl pH 7.5, 150 mM NaCl, 1% Triton X-100, 1% sodium deoxycholate, 0.1% SDS) and centrifugation at 100,000g. We performed western blotting on equal amounts of sample and detected TRESK and  $\beta$ -actin with rabbit polyclonal antibodies to mouse-K<sub>2</sub>P<sub>18.1</sub> (TRESK) (Alamone, APC-122) and  $\beta$ -actin-specific antibodies (Abcam, ab6276), respectively. We retrieved matched fixed and frozen samples from a trigeminal ganglion from a 54-year-old individual with motor neuron disease and no history of migraine from the Thomas Willis Oxford Brain Collection. Frozen sections were cut at 12  $\mu$ m and mounted on Superfrost slides (Thermo Scientific Gerhard Menzel) and TRESK was visualized with TRESK-specific polyclonal antibody (Santa Cruz, sc-51237) and Vectastain ABC kit (Vector Labs), with 3,3'-diaminobenzidine (Vector Labs) as chromogen. We ran negative controls in parallel omitting the primary antibody.

**Electrophysiological characterization of TRESK channels.** We subcloned the human *KCNK18* gene into the oocyte expression vector pBF and created the F139WfsX24 mutation by site-directed mutagenesis, confirmed by automated sequencing. We microinjected *in vitro*-transcribed WT or mutant mRNAs into *Xenopus* oocytes in a 50-nl total volume (**Supplementary Methods**). We recorded whole-cell currents 18–24 h after injection (20–22 °C) using the two-electrode voltage clamp method (Geneclamp 500B, Axon Instruments). We typically measured TRESK currents in low K<sup>+</sup> solution, at the end of 1-s-long voltage steps from a holding potential of –80 mV delivered in 20 mV increments from –120 mV to 60 mV. For the steady-state current-voltage relationships, we determined peak currents at the end of the 1-s pulse and plotted as a function of membrane potential. For the experiments with ionomycin, we measured TRESK currents in high K<sup>+</sup> solution at the end of 300-ms-long voltage steps from 0 mV to –100 mV.

**Statistical analyses.** We obtained allele frequencies of SNPs used in the linkage analysis from the HapMap project. We performed parametric linkage analysis with MERLIN<sup>19</sup>, with a disease allele frequency of 0.0001 and full penetrance. Linkage analysis of tightly linked loci can lead to an excess of false positive results if the markers are in strong linkage disequilibrium, and we therefore used the CLUSTERS option of MERLIN to allow for the linkage disequilibrium.

**Additional methods.** Detailed methodology is described in the **Supplementary Methods**.

28. Lemos, C. *et al.* Familial clustering of migraine: further evidence from a Portuguese study. *Headache* **49**, 404–411 (2009).
29. Colson, N.J., Lea, R.A., Quinlan, S., MacMillan, J. & Griffiths, L.R. Investigation of hormone receptor genes in migraine. *Neurogenetics* **6**, 17–23 (2005).
30. The International Classification of Headache Disorders. 2nd edition. *Cephalalgia* **24** Suppl 1, 9–160 (2004).